Comparative study of hybrid functionals applied to structural and electronic properties of semiconductors and insulators

Yu-ichiro Matsushita,[1,*] Kazuma Nakamura,[1] and Atsushi Oshiyama[1,2]
[1]*Department of Applied Physics, The University of Tokyo, Hongo, Tokyo 113-8656, Japan*
[2]*CREST, Japan Science and Technology Agency, Sanban-cho, Tokyo 102-0075, Japan*
(Received 11 March 2011; revised manuscript received 3 June 2011; published 10 August 2011)

We present a systematic study that clarifies the validity and limitation of current hybrid functionals in density functional theory for structural and electronic properties of various semiconductors and insulators. The three hybrid functionals, PBE0 by Perdew, Ernzerhof, and Burke, HSE by Heyd, Scuseria, and Ernzerhof, and a long-range corrected (LC) functional, are implemented in a well-established plane-wave-basis-set scheme combined with norm-conserving pseudopotentials, thus enabling us to assess the applicability of each functional on an equal footing to the properties of the materials. The materials we have examined range from covalent to ionic materials as well as a rare-gas solid whose energy gaps determined by experiments are in the range of 0.6–14.2 eV, i.e., Ge, Si, $BaTiO_3$, β-GaN, diamond, MgO, NaCl, LiCl, Kr, and LiF. We find that the calculated bulk moduli by the hybrid functionals show better agreement with the experiments than that provided by the generalized-gradient approximation (GGA), whereas the calculated lattice constants by the hybrid functionals and the GGA show comparable accuracy. The calculated energy band gaps and the valence-band widths for the ten prototype materials show substantial improvement using the hybrid functional compared with the GGA. In particular, it is found that the band gaps of the ionic materials as well as the rare-gas solid are well reproduced by the LC-hybrid functional, whereas those of covalent materials are well described by the HSE functional. We also examine exchange effects due to short-range and long-range components of the Coulomb interaction, and we propose an optimum recipe to the short-range and long-range separation in treating the exchange energy.

DOI: 10.1103/PhysRevB.84.075205 PACS number(s): 71.15.Mb, 71.20.Mq

I. INTRODUCTION

The local density approximation (LDA) (Ref. 1) in the density functional theory (DFT) (Ref. 2) has shown a fantastic ability to understand and even predict material properties[3] in spite of its relatively simple treatment of the exchange-correlation energy $E_{\rm XC}[n]$ as a functional of the electron density $n(\boldsymbol{r})$; e.g., for many materials, lattice and elastic constants are generally reproduced. The deviations from experimental values are within less than 1%–2% and several percent, respectively, in the LDA. Yet the LDA fails to describe some properties, including ground-state magnetic orderings even for bulk iron[4] and for some transition-metal oxides.[5] It also tends to overestimate the bonding strength, leading to an absolute error of molecular atomization energies.[6]

Some of the limitations of the LDA are remedied by the generalized-gradient approximation (GGA), in which the exchange-correlation energy is expressed in terms of not only the electron density but also its gradient. The molecular atomization energies are calculated with the error of several tenths of an electron volt,[7] and the ground state of the bulk iron is correctly predicted to be a ferromagnetic body-center phase.[4] The prevailing functional form of the GGA (PBE) (Ref. 8) generally provides better accuracy for structural properties of a variety of solids and activation energies in chemical reactions than the LDA does. In particular, a revised form of PBE (PBEsol) (Ref. 9) has been reported to give even better results for structural properties of solids.

The local (LDA) and semilocal (GGA) approximations are still insufficient to describe some of the important properties, however. The ground states of strongly correlated materials are incorrectly predicted and the energy band gaps of most semiconductors and insulators are substantially underestimated. The meta-GGA scheme[10–12] extending the exchange-correlation functionals with inclusion of the kinetic energy density further improves the LDA and GGA results for molecular systems[13] but does not succeed in remedying the above failures in condensed matter.

The failure of the LDA and the GGA is occasionally discussed in terms of the self-interaction error (SIE).[14,15] An electron is under the electrostatic potential due to other electrons. Yet the expression of the electrostatic potential in the (semi) local approximations includes the spurious interaction with the electron itself. When we consider the Hartree-Fock (HF) exchange potential with Kohn-Sham orbitals, this spurious self-interaction is cancelled by a term in the exchange potential. In the (semi) local expression of the exchange potential, however, this cancellation is incomplete so that each electron is affected by the self-interaction. This SIE causes delocalization of the electron, predicting the incorrect fractional-charged ground state of, e.g., H_2^+ with large nucleus separation.[15] Several schemes to correct the SIE are proposed and their capabilities have been examined for molecular systems.[16–19]

The SIE affects the band gaps substantially. The band gap ΔE_g is formally defined as the ionization energy subtracted by the electron affinity so that $\Delta E_g = E(N+1) + E(N-1) - 2E(N)$, where $E(N)$ is the total energy of the N-electron system. In DFT with the exact exchange-correlation energy, the band gap is expressed as the difference between the highest occupied Kohn-Sham level $\varepsilon_{N+1}(N+1)$ of the $(N+1)$-electron system and its counterpart of the N-electron system $\varepsilon_N(N)$, i.e., $\Delta E_g = \varepsilon_{N+1}(N+1) - \varepsilon_N(N)$.[20–23] When we introduce a fractional electron system with $N+f$ electrons as a mixed state of real integer-electron systems, then the

total energy $E(N+f)$ becomes linear for $0 < f < 1$ and shows discontinuity at the integer value N for finite-gap systems. Using Janak's theorem,[24] which relates the Kohn-Sham level to the derivative of the total energy as $\varepsilon_{N+1}(N+f) = \partial E(N+f)/\partial f$, the linearity of $E(N+f)$ leads to the constant $\varepsilon_{N+1}(N+f)$ as a function of f. In the (semi) local approximations, however, the Kohn-Sham level $\varepsilon_{N+1}(N+f)$ [$\varepsilon_N(N-f)$] increases (decreases) with increasing f due to the self-interaction, leading to the concave shape of $E(N+f)$. This may cause an underestimate of the energy gap.[19,25,26]

The HF approximation (HFA) is free from the self-interaction. Yet the calculated band gaps in the HFA are substantially overestimated due to the lack of the correlation energy. An approach intended to remedy the issue called the optimized effective potential,[27] which is incorporated in DFT (Refs. 28–30), is still in an immature stage in view of applications to polyatomic systems.

Hence the hybrid functionals combining the LDA or the GGA with the HFA may be effective to break the limitation of the semilocal approximations. The hybrid approach began in empirical ways: The HF-exchange energy was mixed with the LDA exchange-correlation energy in the half and half way[31] and then three mixing parameters were introduced[32] to mix the LDA, GGA, and HFA energies; the latter scheme is called B3LYP and has been widely used to clarify the thermochemical properties of molecules.[33] A rationale for the hybrid functional is provided[34] in light of the adiabatic-connection theorem,[35]

$$E_{\mathrm{XC}}[n] = \int_0^1 d\lambda\, E_{\mathrm{XC},\lambda}\,, \tag{1}$$

where

$$E_{\mathrm{XC},\lambda} = \langle\Psi_\lambda|\hat{V}_{ee}|\Psi_\lambda\rangle - \frac{e^2}{2}\int d^3r \int d^3r' \frac{n(\boldsymbol{r})n(\boldsymbol{r}')}{|\boldsymbol{r}-\boldsymbol{r}'|} \tag{2}$$

is the energy of the exchange and correlation in a system, where the electron-electron interaction $\hat{V}_{ee} = (e^2/2)\sum_{ij} 1/|\boldsymbol{r}_i - \boldsymbol{r}_j|$ is reduced by the factor λ but the external potential $v_\lambda(r)$ is added to reproduce the electron density $n(\boldsymbol{r})$ of the real system ($\lambda = 1$). Here Ψ_λ is the ground-state many-body wave function. By assuming that $E_{\mathrm{XC},\lambda}$ is the fourth polynomial of λ with particular asymptotic forms for $\lambda = 0$ and 1, Perdew, Ernzerhof, and Burke have proposed a parameter-free hybrid functional called PBE0,[34] in which the HF and PBE exchange energies are mixed with the ratio of 1 : 3. Its applicability has been examined for molecular systems.[36,37]

Screening of the Coulomb potential is effective in polyatomic systems. Hence it may be appropriate to apply the nonlocal HF-exchange operator only to the short-range part of the Coulomb potential.[38,39] This is conveniently done by introducing the error function splitting the Coulomb potential into short-range and long-range components.[40] The hybrid functional, which is constructed in this way from the PBE0 functional, was proposed by Heyd, Sucseria, and Ernzerhof (HSE).[39] This treatment reduces computational cost substantially and opens a possibility to apply the hybrid functionals to condensed matter. The structural properties as well as the band gaps of several solids have been calculated, and significant improvements on semilocal functionals have been achieved.[41–50]

On the other hand, the effects of the exchange interaction for the long-range component of the Coulomb potential are certainly important[40,51,52] in view of reducing the SIE. Hirao and his collaborators have proposed a long-range corrected (LC) functional in which the long-range component is treated by the HF exchange energy and the short-range component is treated by the LDA exchange energy.[53] They have applied the scheme to various molecular systems and obtained relatively successful results.[54–57] Further application of the LC functional combined with the GGA to molecular systems and its comparison with other functionals has been done, and the applicability of the LC functional has been recognized.[58–60]

The LC functional has also been applied to structural properties and band gaps of several condensed matters, and the results are compared with those obtained from other functionals.[61]

At the present stage, several hybrid functionals have been implemented in different packages, and the assessment of the validity of each functional has been done mainly to molecular systems, although the applicability of the PBE0 and HSE functionals to condensed matters has been examined using the Gaussian-orbital basis sets.[41,42,44–46,49]

The structural and electronic properties, such as lattice constants, bulk moduli, and also the band gaps of condensed matters, are obtained only after careful examinations of various calculation parameters. Obviously, numerical precision should not be neglected. In order to assess the validity of each hybrid functional, it is thus imperative to perform the computation in a single reliable calculation scheme. Furthermore, the split of the Coulomb potential into the short-range and long-range parts requires another parameter ω being the exponent of the error function. The ω dependence of the results should certainly be examined for better understanding and further improvements on the hybrid functionals.

The aim of the present paper is to implement several important hybrid functionals in the well-established plane-wave-basis total-energy band-structure calculation code and examine the validity and limitation of each functional. A plane-wave code we adopt in this work is the Tokyo Ab initio Program Package (TAPP).[62–65] We have calculated lattice constants, bulk moduli, band gaps, and bandwidths of various semiconductors and insulators with the PBE0, HSE, and LC hybrid functionals as well as the (semi) local GGA functional. Comparison of the obtained results unequivocally elucidates the validity and the limitation of the hybrid functionals.

In Sec. II, we briefly describe each of the hybrid functionals used in the present paper. Section III presents details of our computational scheme. The calculated results are shown in Sec. IV, and our finding is summarized in Sec. V.

II. HYBRID EXCHANGE-CORRELATION FUNCTIONALS

In this section, we briefly describe the three hybrid functionals, PBE0, HSE, and LC, the applicability of which is examined in this paper.

A. PBE0 functional

Perdew, Burke, and Ernzerhof have proposed[34] a polynomial form for $E_{\mathrm{XC},\lambda}$ as

$$E_{\mathrm{XC},\lambda} = E_{\mathrm{XC},\lambda}^{\mathrm{DFT}} + \left(E_X^{\mathrm{HF}} - E_X^{\mathrm{DFT}}\right)(1-\lambda)^{n-1}, \tag{3}$$

where $E_X^{\rm HF}$ and $E_X^{\rm DFT}$ are the exchange energies obtained by the HFA and a certain (semi) local approximation in DFT, respectively. Here $E_{{\rm XC},\lambda=1}^{\rm DFT}$ is the energy of the exchange and correlation defined as Eq. (2) and obtained by the (semi) local approximation in DFT. This formula infers that the (semi) local approximation in DFT is a good approximation to $E_{{\rm XC},\lambda}$ for $\lambda = 1$. When $\lambda = 0$, this formula is equal to $E_x^{\rm HF}$ since $E_{{\rm XC},\lambda}^{\rm DFT} = E_x^{\rm DFT}$ for $\lambda = 0$.

From Eqs. (1) and (3), we obtain

$$E_{\rm XC} = E_{\rm XC}^{\rm DFT} + \frac{1}{n}\left(E_X^{\rm HF} - E_X^{\rm DFT}\right). \tag{4}$$

Relying on the fourth-order Möller-Plesset perturbation theory applied for molecular systems, it is argued that $n = 4$ is the best choice.[34] Using the PBE functional[8] as the approximation in DFT in Eq. (4), the PBE0 hybrid functional is given by

$$E_{\rm XC} = E_{\rm XC}^{\rm PBE} + \tfrac{1}{4}\left(E_X^{\rm HF} - E_X^{\rm PBE}\right), \tag{5}$$

leading to the mixing of 25% HF exchange and 75% PBE exchange.

B. HSE functional

Heyd, Sucseria, and Ernzerhof have proposed[39] a different hybrid functional in which the long-range part of the HF-exchange energy is treated by the semilocal approximation in DFT and the short-range part is calculated exactly. The actual procedure is conveniently done by splitting the Coulomb potential as

$$\frac{1}{r} = \frac{{\rm erfc}(\omega r)}{r} + \frac{{\rm erf}(\omega r)}{r}, \tag{6}$$

and applying the first term only, i.e., the screened Coulomb potential, to the HF-exchange energy. The second term to the exchange energy is calculated with the GGA. Adopting the mixing ratio in PBE0, the HSE hybrid functional the becomes

$$E_{\rm XC}^{\rm HSE} = E_{\rm XC}^{\rm PBE} + \tfrac{1}{4}\left(E_X^{\rm HF,SR} - E_X^{\rm PBE,SR}\right). \tag{7}$$

$E_X^{\rm HF,SR}$ is the Fock-type double integral with the screened Coulomb potential. There is some complexity to dividing the PBE exchange energy $E_X^{\rm PBE}$ into the short-range part $E_X^{\rm PBE,SR}$ and the long-range part $E_X^{\rm PBE,LR}$. The dividing procedure will be shown in Sec. III C.

Another ambiguous factor is the parameter ω in Eq. (6), which defines the short-range and the long-range parts of the Coulomb potential. Several efforts to determine the optimum value of ω have been done by examining the calculated results for molecular systems,[39,41,58,66] and the recommended values are in the range $\omega \sim 0.1$–$0.3a_B^{-1}$ (a_B denotes the Bohr radius).

Examining the ω dependence of the calculated results for condensed matters is one of our aims in this paper.

C. LC functional

The HSE functional partly removes the SIE by incorporating the HF-exchange energy in the PBE functional. Yet the cancellation of the Hartree potential and the exchange potential is absent in the long-range part. This may cause erroneous description of, e.g., the Rydberg states in isolated polyatomic systems or properties of charge-transfer systems. To remedy this point, application of the long-range part of the Coulomb potential to the HF-exchange energy is necessary.[40] The long-range corrected (LC) functional has been proposed based on this viewpoint,[53] being expressed as

$$E_{\rm XC}^{\rm LC} = E_{\rm XC}^{\rm DFT} + \left(E_X^{\rm HF,LR} - E_X^{\rm DFT,LR}\right), \tag{8}$$

with $E_X^{\rm HF,LR}$ being the Fock-type double integral with the long-range part of the Coulomb potential [the second term of Eq. (6)]. For the DFT part, several approximations, including the LDA,[58,61], the PBE,[55,58,59] and other GGA (Ref. 53) or meta-GGA (Ref. 58) forms, are adopted in Eq. (8) and their validity is examined. It is argued that PBE combined in the LC hybrid scheme provides good accuracy for molecular properties.[59,67] As in the HSE scheme, there is some complexity to extracting the long-range component of the exchange energy of the DFT part, $E_X^{\rm DFT,LR}$.

The parameter ω in Eq. (6) affects the results substantially. By examining the results for molecular systems, the values ranging from $\omega = 0.25$ to 0.5 are argued to be optimum.[53,58] By applying the LDA in the LC-hybrid scheme to structural properties of solids, the value $\omega = 0.5$ is found to produce reasonable results.[61] It is of interest to investigate the appropriate value of ω in the application of PBE in the LC-hybrid scheme to structural properties and band gaps of condensed matter.

III. COMPUTATIONAL DETAILS

In this section, we describe our implementation of the hybrid functionals in the plane-wave basis-set total-energy band-structure calculation code, TAPP.[62–65] Nuclei and core electrons are simulated by either norm-conserving[68] or ultrasoft[69] pseudopotentials in the TAPP code. Nonlocality of the HF-exchange potential generally increases computational cost tremendously in the application to condensed matter. We have circumvented this problem using the fast-Fourier transform (FFT), as explained below. The long-range nature of the Coulomb potential leads to singularity of its Fourier transform at the origin. This causes difficulty in numerical integration over the Brillouin zone (BZ) to obtain the HF-exchange energy in the PBE0 and LC schemes. We adopt here a simple truncation scheme to overcome the problem. Finally, we explain how to divide the exchange energy in the PBE functional to the short-range and long-range components.

A. Calculation of $E_X^{\rm HF}$ by FFT

The HF-exchange energy $E_X^{\rm HF}$ in condensed matter (crystal) is written as

$$E_X^{\rm HF} = -\frac{1}{2}\sum_{n\mathbf{k}}\sum_{n'\mathbf{k}'} f_{n\mathbf{k}} f_{n'\mathbf{k}'} J_{n\mathbf{k}n'\mathbf{k}'}\ , \tag{9}$$

where $f_{n\mathbf{k}}$ is the occupation number, and $J_{n\mathbf{k}n'\mathbf{k}'}$ is given by

$$J_{n\mathbf{k}n'\mathbf{k}'} = \int\int d\mathbf{r}\, d\mathbf{r}' \frac{\phi_{n\mathbf{k}}^*(\mathbf{r})\phi_{n'\mathbf{k}'}^*(\mathbf{r}')\phi_{n\mathbf{k}}(\mathbf{r}')\phi_{n'\mathbf{k}'}(\mathbf{r})}{|\mathbf{r}-\mathbf{r}'|}\ . \tag{10}$$

Here $\phi_{n\mathbf{k}}(\mathbf{r})$ is the Bloch-state orbital with the band index n and the wave vector $\mathbf{k}$. The orbital $\phi_{n\mathbf{k}}(\mathbf{r})$ is obtained by solving self-consistently the Euler equation (Kohn-Sham equation) in which the exchange-correlation potential is given

by the functional derivative of the hybrid exchange-correlation energy. The sums over $\mathbf{k}$ and n are taken for the occupied states.

Our algorithm to compute the integral $J_{n\mathbf{k}n'\mathbf{k}'}$ in the plane-wave-basis code is as follows: Eq. (10) is written as

$$J_{n\mathbf{k}n'\mathbf{k}'} = \int d\mathbf{r}\, d\mathbf{r}' \frac{u^*_{n\mathbf{k}}(\mathbf{r}) u^*_{n'\mathbf{k}'}(\mathbf{r}') u_{n\mathbf{k}}(\mathbf{r}') u_{n'\mathbf{k}'}(\mathbf{r})}{|\mathbf{r}-\mathbf{r}'|} \times e^{-i(\mathbf{k}-\mathbf{k}')\cdot\mathbf{r}} e^{i(\mathbf{k}-\mathbf{k}')\cdot\mathbf{r}'}, \tag{11}$$

with $u_{n\mathbf{k}}(\mathbf{r}) = \exp(-i\mathbf{k}\cdot\mathbf{r})\phi_{n\mathbf{k}}(\mathbf{r})$. In the plane-wave basis-set scheme, the reciprocal-lattice vectors $\mathbf{G}$ are used to represent the periodic wave function as $u_{n\mathbf{k}}(\mathbf{r}) = \sum_{\mathbf{G}} e^{i\mathbf{G}\cdot\mathbf{r}} u_{n\mathbf{k}}(\mathbf{G})$. We then obtain

$$J_{n\mathbf{k}n'\mathbf{k}'} = \sum_{\mathbf{G}\mathbf{G}'\mathbf{G}''} \frac{4\pi}{|\mathbf{k}'-\mathbf{k}+\mathbf{G}'-\mathbf{G}''|^2} u_{n\mathbf{k}}(\mathbf{G})^* u_{n'\mathbf{k}'}(\mathbf{G}')^* \times u_{n\mathbf{k}}(\mathbf{G}'') u_{n'\mathbf{k}'}(\mathbf{G}+\mathbf{G}'-\mathbf{G}''). \tag{12}$$

When we compute Eq. (10) directly, the calculation costs of $J_{n\mathbf{k}n'\mathbf{k}'}$ and $E_{\mathrm{x}}^{\mathrm{HF}}$ are $O(N_{\mathbf{G}}^3)$ and $O(N_{\mathrm{band}}^2) \times O(N_{\mathbf{k}}^2) \times O(N_{\mathbf{G}}^3)$, respectively, where $N_{\mathbf{G}}$ is the total number of the reciprocal vectors, $N_{\mathbf{k}}$ is the total number of sampling $\mathbf{k}$ points in the BZ, and N_{band} is the total number of the occupied bands. The number of $N_{\mathbf{G}}$ is much bigger than either N_{band} or $N_{\mathbf{k}}$. Hence the order $N_{\mathbf{G}}^3$ is computationally demanding.

We reduce this computational cost by using FFT. We first define the overlap density between states $(n\mathbf{k})$ and $(n'\mathbf{k}')$ as

$$n_{n\mathbf{k}n'\mathbf{k}'}(\mathbf{r}) = u^*_{n\mathbf{k}}(\mathbf{r}) u_{n'\mathbf{k}'}(\mathbf{r}). \tag{13}$$

Using this quantity, we obtain

$$J_{n\mathbf{k}n'\mathbf{k}'} = \int d\mathbf{r}\, d\mathbf{r}' \frac{n_{n\mathbf{k}n'\mathbf{k}'}(\mathbf{r}) n_{n\mathbf{k}n'\mathbf{k}'}(\mathbf{r})^*}{|\mathbf{r}-\mathbf{r}'|} \times e^{-i(\mathbf{k}-\mathbf{k}')\cdot\mathbf{r}} e^{i(\mathbf{k}-\mathbf{k}')\cdot\mathbf{r}'}. \tag{14}$$

We note that, since $u_{n\mathbf{k}}(\mathbf{r})$ has unit-cell periodicity, the overlap density also has the same periodicity. Using the Fourier transformation of the overlap density $n_{n\mathbf{k}n'\mathbf{k}'}(\mathbf{r})$, Eq. (14) is rewritten as

$$J_{n\mathbf{k}n'\mathbf{k}'} = \sum_{\mathbf{G}} \frac{4\pi}{|\mathbf{k}-\mathbf{k}'-\mathbf{G}|^2} |n_{n\mathbf{k}n'\mathbf{k}'}(\mathbf{G})|^2. \tag{15}$$

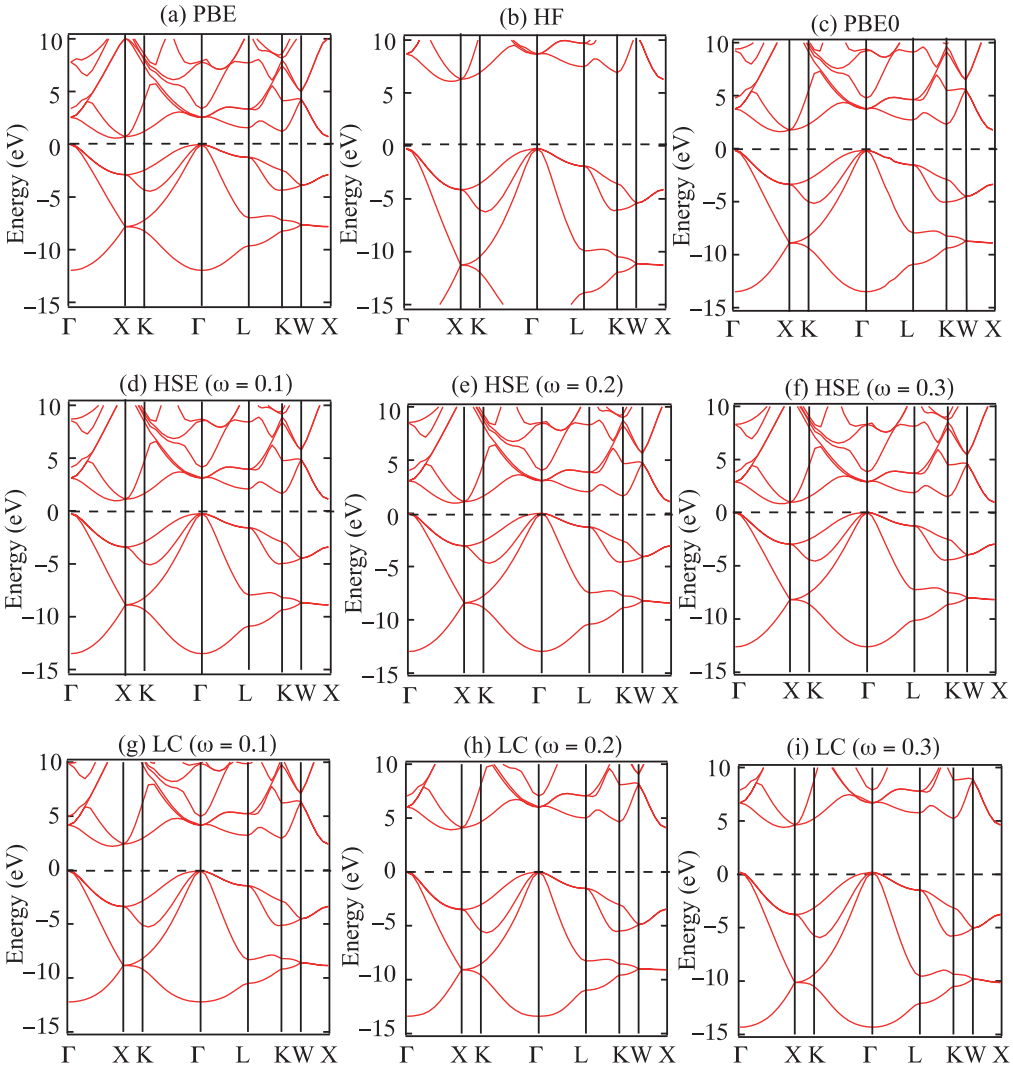

FIG. 1. (Color online) Calculated energy bands of Si with PBE (a), HF (b), PBE0 (c), HSE (d)–(f), and LC (g)–(i) exchange-correlation functionals. The origin of the energy is set at the valence-band top.

Since the $n_{n\mathbf{k}n'\mathbf{k}'}(\mathbf{G})$ can be calculated outside the summation loop in Eq. (15), the total calculation cost for $J_{n\mathbf{k}n'\mathbf{k}'}$ is $O(N_\mathbf{G} + N_\mathbf{G} \ln N_\mathbf{G})$. The computational cost of E_x^HF becomes $O(N_\mathrm{band}^2) \times O(N_\mathbf{k}^2) \times O(N_\mathbf{G} + N_\mathbf{G} \ln N_\mathbf{G})$. Considering the scaling as $N_\mathbf{G} \propto N_\mathrm{atom}$, $N_\mathrm{band} \propto N_\mathrm{atom}$, and $N_\mathrm{k} \propto 1/N_\mathrm{atom}$ with N_atom the number of atoms in the unit cell, the computational cost above is proportional to $N_\mathrm{atom} + N_\mathrm{atom} \ln N_\mathrm{atom}$.

B. Treatment of divergence in the Coulomb interaction

The Fourier transform $v(\boldsymbol{q})$ of the Coulomb potential $v(\boldsymbol{r})$ diverges at the long-wavelength limit $\boldsymbol{q} \to 0$. Calculations of electrostatic energies thus require careful treatment, and the well-known Ewald summation is the typical example. In calculating nonlocal exchange energies in condensed matter, more careful treatment is necessary. We need to perform the BZ integration in evaluation of the exchange energy in Eq. (9). The integration is usually performed by the summation with weighting factors of the integrand at finite discrete $\boldsymbol{k}$ points, and thus we encounter a difficulty in evaluating the integral accurately by picking up the singular behavior of the Fourier transform of the Coulomb potential. There are several ways to overcome this difficulty. One is the auxiliary-function approach: An auxiliary function that has the same singular behavior but is integrable is subtracted so that the summation can be done properly and the remaining term is obtained analytically.[70–72] An alternative way, which we adopt in the present paper, is simpler: We make the Coulomb potential truncated at R_c and then examine the convergence by numerically increasing R_c.[73] Namely, we replace the Coulomb potential with a truncated potential,

$$\tilde{v}(\boldsymbol{r}) = \begin{cases} \frac{1}{|\boldsymbol{r}|} & \text{if } |\boldsymbol{r}| \leqslant R_c, \\ 0 & \text{otherwise,} \end{cases} \tag{16}$$

with a cutoff radius R_c. What we need is of course converged quantities with $R_c \to \infty$. The truncated potential produces its nondivergent Fourier transform,

$$\tilde{v}(\boldsymbol{q}) = \frac{4\pi}{|\boldsymbol{q}|^2}[1 - \cos(|\boldsymbol{q}|R_c)] \,. \tag{17}$$

Convergence of required quantities with respect to R_c is combined with the number of sampling $\boldsymbol{k}$ points in the BZ

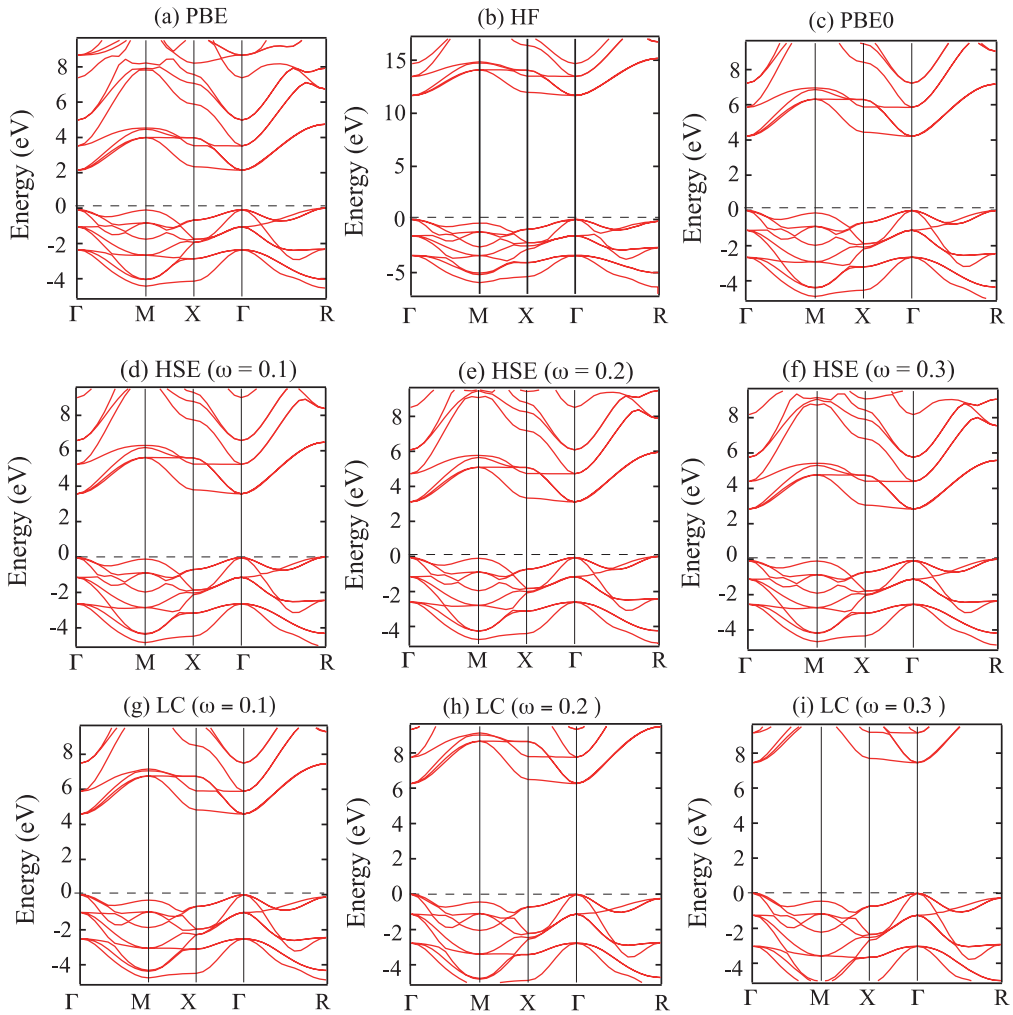

FIG. 2. (Color online) Calculated energy bands of $BaTiO_3$ with PBE (a), HF (b), PBE0 (c), HSE (d)–(f), and LC (g)–(i) exchange-correlation functionals. The origin of the energy is set at the valence-band top. Note that the vertical scale in (b) is different from those in the other panels.

integration. The number N_k of sampling $\boldsymbol{k}$ points required should increase with increasing R_c. We need to know the converged values with increasing both R_c and N_k. The process to check this convergence in the two-parameter space can be done conveniently by introducing a certain relation between R_c and N_k. We set up a relation, $N_k = 4\pi R_c^3/(3\Omega_c)$, where Ω_c is the unit-cell volume, and we examine the convergence of the exchange energy by increasing N_k and equivalently R_c. We have found that the values of R_c, which are four to six times the dimension of the primitive unit cell, are enough to assure the converged exchange energies in ten materials calculated in the present paper.

C. Calculations of $E_x^{\mathrm{PBE,SR}}$ and $E_x^{\mathrm{BBE,LR}}$

We next describe how to obtain the short-range and long-range parts in the PBE-exchange energy, following Ref. 74. The original expression for the PBE-exchange energy is given by

$$E_x^{\mathrm{PBE}} = \int d\mathbf{r}\epsilon_x^{\mathrm{unif}}[n(\mathbf{r})]n(\mathbf{r})F_x^{\mathrm{PBE}}(s)\,, \tag{18}$$

where $\epsilon_x^{\mathrm{unif}}[n]$ is the exchange energy of the homogeneous electron gas with the electron density n, and $F_x^{\mathrm{PBE}}(s)$ is an enhanced factor due to a density gradient $s=|\nabla n|/(2k_F n)$ with the Fermi wave number $k_F=(3\pi^2 n)^{1/3}$. The enhanced factor is written in an integral form

$$F_x^{\mathrm{PBE}}(s) = -\frac{8}{9}\int_0^\infty dy\, y J_x^{\mathrm{PBE}}(s,y), \tag{19}$$

where $y = k_F r$ is a dimensionless quantity and $J_x^{\mathrm{PBE}}(s,y)$ describes an exchange-hole density at the distance r. Heyde, Scuseria, and Ernzerhof[39] proposed an expression for the short-range PBE-exchange functional, where the original Coulomb interaction $1/r$ is modified to a screened form $\mathrm{erfc}(\omega r)/r$. This modification leads to an enhanced factor somewhat different from the original expression of Eq. (19) as

$$F_x^{\mathrm{PBE,SR}}(s,\omega) = -\frac{8}{9}\int_0^\infty dy\, y J_x^{\mathrm{PBE}}(s,y)\mathrm{erfc}\left(\frac{\omega y}{k_F}\right). \tag{20}$$

The short-range exchange energy is given with this enhanced factor as

$$E_x^{\mathrm{PBE,SR}}(\omega) = \int d\mathbf{r}\,\epsilon_x^{\mathrm{unif}}[n(\mathbf{r})]n(\mathbf{r})F_x^{\mathrm{PBE,SR}}(s,\omega). \tag{21}$$

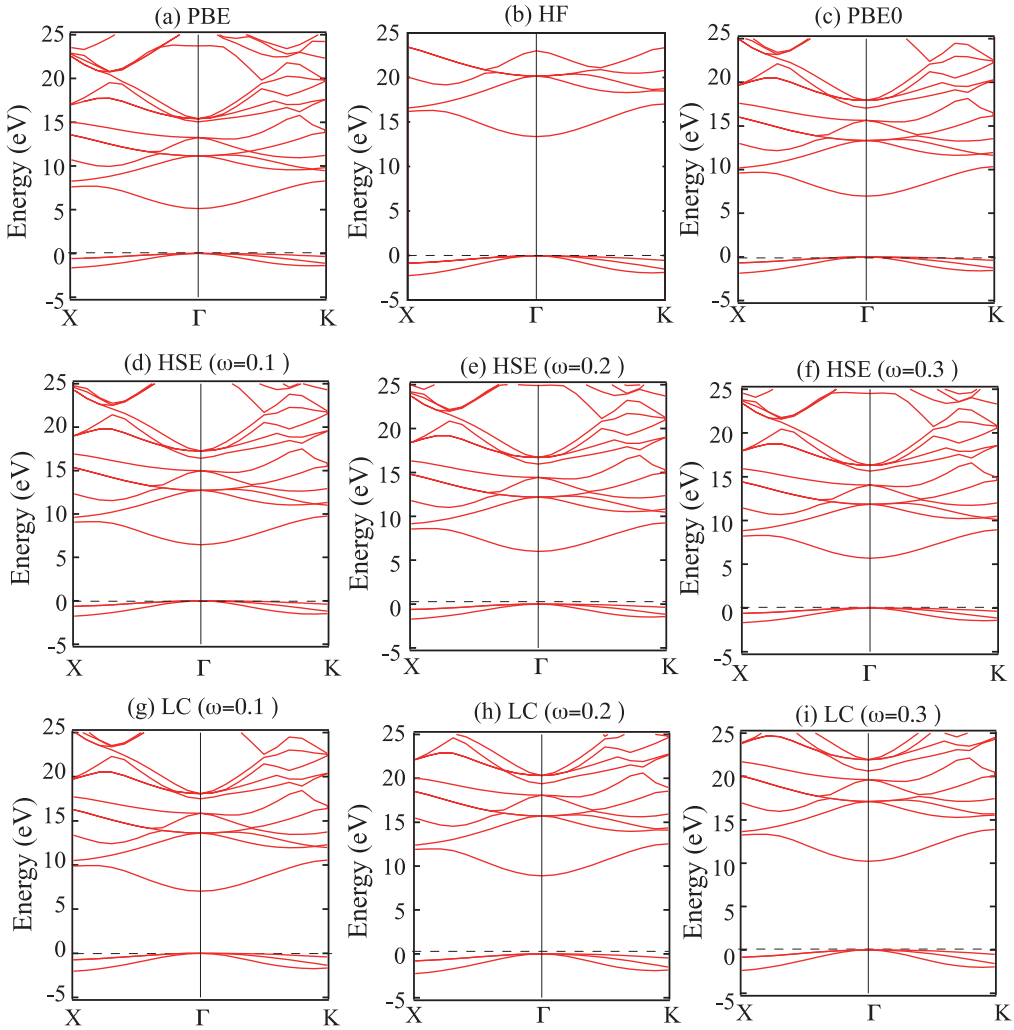

FIG. 3. (Color online) Calculated energy bands of NaCl with PBE (a), HF (b), PBE0 (c), HSE (d)–(f), and LC (g)–(i) exchange-correlation functionals. The origin of the energy is set at the valence-band top.

The long-range PBE-exchange term is defined by subtracting the short-range part in Eq. (21) from the original one in Eq. (18) as

$$E_x^{\mathrm{PBE,LR}}(\omega) = E_x^{\mathrm{PBE}} - E_x^{\mathrm{PBE,SR}}(\omega). \quad (22)$$

Implementation details for these calculations can also be found in Ref. 75.

D. Calculation conditions

We generate norm-conserving pseudopotential to simulate nuclei and core electrons, following a recipe by Troullier and Matins.[68] The core radius r_c is an essential parameter to determine transferability of the generated pseudopotential. We have examined the r_c dependence of the calculated structural properties of benchmark materials and adopted the pseudopotentials generated with the following core radii in this paper: 0.85 Å for Si $3s$, and 1.16 Å for Si $3p$, 1.06 Å for Ge $4s$ and $4p$, 1.06 Å for Ga $4s$ and $4p$, and 1.48 Å for Ga $4d$, 0.64 Å for N $2s$ and $2p$, 0.85 Å for C $2s$ and $2p$, 0.79 Å for O $2s$ and $2p$, 1.38 Å for Na $2s$ and $2p$, 1.16 Å for Cl $3s$ and $3p$, 0.95 Å for Li $2s$, 0.64 Å for F $2s$ and $2p$, 1.59 Å for Ba $5s$, $5p$, and $5d$, 1.32 Å for Mg $2s$ and $2p$, and 1.38 Å for Ti $3d$ and $4s$, and 1.43Å for Ti $4p$, 1.48 Å for Kr $4s$ and 1.37 Å for Kr $4p$.

The pseudopotentials are generated by the (semi) local approximations in DFT. This means that the HF-exchange energy between core and valence states is neglected. Yet we have found that the calculated energy bands obtained with the pseudopotentials generated in the LDA and the GGA are essentially identical to each other, implying that the treatment of the exchange-correlation energy in generating pseudopotentials has minor effects.

The partial core correction[76] is not included in our calculations. This is partly because magnetic properties are not considered in the present work. However, to assure the accuracy of the structural properties, we regard some of the core orbitals as valence orbitals and include them explicitly in the pseudopotential generation: Such orbitals included as valence states are $2s$ and $2p$ orbitals of Na and $2s$ and $2p$ orbitals of Mg.

Appropriate choice of cutoff energies E_{cut} in the plane-wave-basis set, which is related to the hardness of the adopted norm-conserving pseudopotentials, is a principal ingredient to ensure the accuracy of the results. We have examined the convergence of structural properties and band gaps with respect to E_{cut} and reached the following well-converged values with E_{cut} for each material: 25 Ry for Si and Ge; 36 Ry for Kr; 64 Ry for $BaTiO_3$; and 100 Ry for diamond, GaN, MgO, NaCl, LiCl, and LiF. The remaining important ingredient to ensure the accuracy of our assessment of each hybrid functional is the sampling $\boldsymbol{k}$ points for the BZ integration. We have adopted the scheme by Monkhorst and Pack in which the BZ is divided by an equally spaced mesh. After careful examination, we have found that $4 \times 4 \times 4$ sampling $\boldsymbol{k}$ points are enough to ensure the accuracy of the total energies and energy bands in the ten materials. The results are confirmed by repeating the calculations with $6 \times 6 \times 6$ sampling $\boldsymbol{k}$ points.

IV. RESULTS AND DISCUSSION

We have performed total-energy electronic-structure calculations using PBE, HF, PBE0, HSE, and LC exchange-correlation functionals for ten materials, including covalent semiconductors, ionic insulators, dielectric compounds, and a rare-gas solid, i.e., Si, Ge, GaN, diamond, MgO, NaCl, LiCl, LiF, $BaTiO_3$, and Kr. The calculated results elucidate the capability and limitation of each functional in discussing the electronic and structural properties of these prototype materials. We first present the calculated electron states of these materials and compare them with experimental results in Sec. IV A. Then we present the results of structural optimization in Sec. IV B.

A. Energy bands and gaps

Figure 1 shows calculated band structures of Si with five exchange-correlation functionals. For the HSE and LC functionals, the band structures with different choices of ω [0.1, 0.2, and $0.3(a_B^{-1})$] in Eq. (6) are shown. The overall features of the band structures obtained by the five functionals are similar to each other. Yet the bandwidths and the fundamental gaps are different quantitatively. When the ratio of the HF exchange to the total-exchange functional is large, the resulting bandwidth and gap become large; these quantities become larger in the order of PBE, PBE0, HSE, LC, and HF. Notice that the band gaps obtained by the LC functional are always larger than those by the HSE functional, indicating that the correction to the long-range part of the exchange potential tends to make the band gap large.

We also show the calculated energy bands of the dielectric compound $BaTiO_3$ and the ionic insulator NaCl in Figs. 2 and 3, respectively. We find the general tendency similar to that in Si, i.e., the overall features of the energy bands are insensitive to the difference in the functionals; the LC functional provides larger energy gaps compared with the HSE functional.

Tables I and II summarize the calculated bandwidths and band gaps for the ten materials. To assess the validity of each functional, it is convenient to introduce two quantities: the mean relative error (MRE), which is the mean of the calculated value minus the experimental value over the ten materials, and the mean absolute relative error (MARE), which is the mean of the absolute value of the difference between the calculated and the experimental values over the ten materials. The MRE is a measure of under- or overestimates of the experimental values, since each functional predicts either smaller or larger values than the experimental values for most of the ten materials. On the other hand, MARE is a measure of closeness between the calculated and experimental values. In the discussion below, we categorize the ten materials into group I and group II: group I, i.e., diamond, GaN, $BaTiO_3$, Si, and Ge, has covalent characters in which the band gaps are less than 7 eV; group II, i.e., LiF, Kr, NaCl, LiCl, and MgO, consists of ionic solids and a rare-gas solid in which the experimental band gaps are larger than 7 eV.

The calculated bandgap by the PBE functional for each material is substantially smaller than the corresponding experimental value, as is reported in the literature. The calculated MRE for the ten materials is -42.5%. On the other hand, the

TABLE I. Band gaps ϵ_{gap} obtained from PBE, HF, PBE0, HSE, and LC calculations. The ω is a parameter that separates the long-range and short-range parts of the Coulomb interaction (see text). Experimental values are taken from Ref. 80 for Ge, Si, and C; Ref. 42 for β-GaN; Ref. 81 for $BaTiO_3$; Ref. 82 for MgO; Ref. 83 for NaCl; Ref. 84 for Kr; and Ref. 85 for LiCl and LiF. The calculated mean relative error (MRE) and the mean absolute relative error (MARE) with respect to experimental values are also shown in percent. Group I consists of materials having an experimental gap less than 7 eV, while group II consists of materials with a gap of more than 7 eV (see text).

	ϵ_{gap}											
	PBE	HF	PBE0	HSE				LC				Expt.
				$\omega = 0.1$	$\omega = 0.2$	$\omega = 0.3$	$\omega = 0.4$	$\omega = 0.1$	$\omega = 0.2$	$\omega = 0.3$	$\omega = 0.4$	
Ge	0	4.75	1.00	0.76	0.54	0.43	0.27	1.05	2.05	2.66	3.69	0.74
Si	0.61	6.03	1.72	1.20	0.94	0.80	0.73	2.24	3.85	4.19	4.63	1.17
$BaTiO_3$	2.14	11.62	4.21	3.57	3.12	2.83	2.73	4.59	6.26	7.45	8.01	3.2
β-GaN	2.06	8.84	3.51	3.02	2.65	2.42	2.26	3.95	5.58	6.55	7.36	3.30
C	4.01	12.44	5.87	5.28	4.88	4.62	4.45	5.06	6.80	7.95	8.73	5.48
MgO	4.95	14.21	6.99	6.62	6.14	5.79	5.52	6.38	8.33	9.88	11.12	7.7
NaCl	5.13	13.38	6.95	6.46	6.00	5.69	5.49	7.03	8.90	10.22	11.12	8.5
LiCl	6.33	14.85	8.60	8.14	7.67	7.36	7.15	8.53	10.45	11.75	12.66	9.4
LiF	9.70	21.57	12.51	12.02	11.45	11.02	10.68	11.59	13.87	15.65	17.06	14.30
Kr	7.09	15.22	9.14	8.46	7.98	7.68	7.48	9.85	11.75	13.00	13.75	11.65
						All solids						
MARE (%)	42.5	179.7	19.7	12.4	19.9	26.4	31.5	28.2	62.3	88.9	117.4	
MRE (%)	−42.5	179.7	5.7	−9.0	−19.9	−26.4	−31.5	11.1	61.7	88.9	117.4	
						Group I (Ge, Si, $BaTiO_3$, GaN, C)						
MARE (%)	49.1	303.1	25.4	5.8	16.0	25.5	33.2	40.8	119.0	158.8	205.4	
MRE (%)	−49.1	303.1	25.4	0.9	−16.0	−25.5	−33.2	37.8	119.0	158.8	205.4	
						Group II (MgO, NaCl, LiCl, LiF, Kr)						
MARE (%)	35.9	56.3	14.0	19.0	23.9	27.3	29.8	15.6	5.6	18.9	29.4	
MRE (%)	−35.9	56.3	−14.0	−19.0	−23.9	−27.3	−29.8	−15.6	4.4	18.9	29.4	

HFA largely overestimates the band gaps for all ten materials: MRE is 179.7%. The PBE0 functional provides better values. The calculated MRE by the PBE0 for the materials in group I is 25.4%, whereas it gives −14.0 % for the materials in group II.

The HSE and LC functional also provide better agreement of the band gap with the experiments than the PBE does. Furthermore, when we choose optimum values of ω, the HSE and LC results show nice agreement with the experimental values. In the HSE functional, a general trend is the decrease in the band gap with increasing ω. We have found that the value $\omega = 0.1a_B^{-1}$ produces band gaps close to the experimental values within an MRE of 0.9% for the materials in group I.[89]

TABLE II. Valence bandwidth W obtained from PBE, HF, PBE0, HSE, and LC calculations. The ω is a parameter that separates the long-range and short-range parts of the Coulomb interaction (see text). Experimental values are taken from Refs. 77 and 86 for Ge; Refs. 77 and 80 for Si; and Refs. 77, 87, and 88 for C.

	W									
	PBE	HF	PBE0	HSE			LC			Expt.
				$\omega = 0.1$	$\omega = 0.2$	$\omega = 0.3$	$\omega = 0.1$	$\omega = 0.2$	$\omega = 0.3$	
Ge	12.85	18.22	14.50	13.80	13.47	13.11	14.23	15.54	16.36	12.9 ± 0.2
Si	11.95	16.90	13.37	13.28	12.99	12.65	12.19	13.45	14.52	12.5 ± 0.6
$BaTiO_3$	4.53	6.37	5.08	5.03	4.95	4.85	4.85	5.34	5.72	
β-GaN	6.73	8.27	7.20	7.11	7.02	6.93	7.11	7.44	7.91	
C	21.65	30.09	23.64	23.51	23.28	22.96	24.15	25.00	26.19	$24.2 \pm 1, 21 \pm 1$
MgO	4.43	6.16	4.97	4.80	4.70	4.60	5.21	5.56	5.92	
NaCl	1.65	2.24	1.84	1.77	1.71	1.67	2.04	2.25	2.38	
LiCl	2.82	4.33	3.39	3.16	3.16	3.09	3.59	3.91	4.17	
Kr	1.50	1.93	1.61	1.59	1.55	1.52	1.57	1.74	1.85	
LiF	2.83	3.66	3.09	2.96	2.92	2.87	2.94	3.09	3.27	

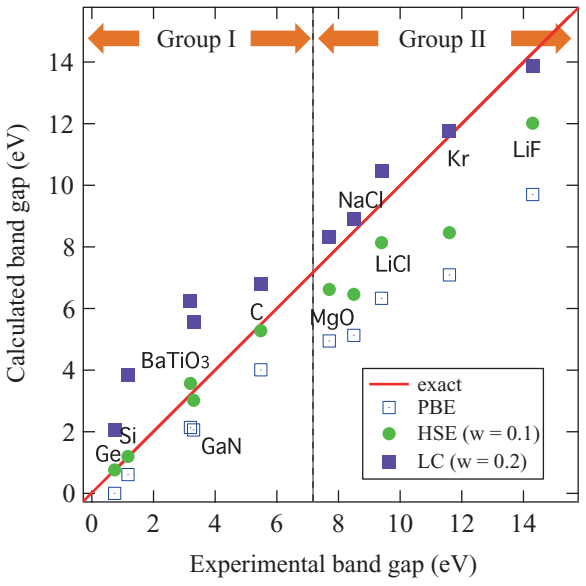

FIG. 4. (Color online) Calculated band gaps obtained from different exchange-correlation functionals: PBE (blank squares), HSE with $\omega = 0.1a_B^{-1}$ (green dots), and LC with $\omega = 0.2a_B^{-1}$ (purple squares), plotted against experimental band gaps. Group I consists of materials having an experimental gap less than 7 eV, while group II is composed of materials with a gap of more than 7 eV.

It produces worse values for the materials in group II. The calculated MRE is −19.0% for the materials in group II, but HSE is still a better approximation than PBE.

The LC functional provides good agreement with the experimental values for the materials in group II: When we choose the optimum value of $\omega = 0.2a_B^{-1}$, the calculated MRE is nicely small, 4.4% for the materials in group II. Yet the LC provides worse values for the materials in group I, showing its limitation as a universally valid approximation.

Figure 4 is a summary of our calculated band gaps by the PBE, HSE, and LC functionals. For HSE and LC, we show the calculated results with the optimum ω values: $\omega = 0.1a_B^{-1}$ for HSE and $\omega = 0.2a_B^{-1}$ for LC. It is clearly shown that the calculated band gaps by hybrid functionals, HSE and LC, are in better agreement with the experimental values than the PBE (GGA) approximation, indicating the promising possibility of the hybrid functionals. The degree of agreement is close to the Green's-function-based GW approximation, in which there are several ambiguities in theoretical treatments.[77–79] However, this figure also shows a limitation in that HSE is reasonably good for only the group I materials, whereas LC is good for only the group II materials.

Our finding here is that HSE is a good approximation for relatively small-gap materials and that LC is a good approximation for the relatively large-gap materials. Screening

TABLE III. Lattice constants a_0 (Å) obtained from PBE, HF, PBE0, HSE, and LC calculations. The ω parameter separates the short-range and long-range parts of the Coulomb interaction (see text). Experimental values are taken from Ref. 42 for Ge, Si, β-GaN, C, and MgO; Refs. 90 and 91 for $BaTiO_3$; Ref. 41 for NaCl, LiCl, and LiF; and Ref. 92 for Kr. The calculated MRE and MARE with respect to experimental values are also shown in percent.

	a_0											
	PBE	HF	PBE0	HSE				LC				Expt.
				$\omega = 0.1$	$\omega = 0.2$	$\omega = 0.3$	$\omega = 0.4$	$\omega = 0.1$	$\omega = 0.2$	$\omega = 0.3$	$\omega = 0.4$	
Ge	5.589	5.574	5.615	5.546	5.556	5.566	5.571	5.579	5.534	5.508	5.490	5.652
Si	5.463	5.387	5.431	5.435	5.441	5.446	5.452	5.459	5.434	5.416	5.403	5.430
$BaTiO_3$	4.139	4.048	4.068	4.102	4.106	4.111	4.116	4.137	4.120	4.102	4.088	4.000
β-GaN	4.539	4.380	4.434	4.455	4.457	4.441	4.461	4.502	4.511	4.491	4.452	4.520
C	3.563	3.485	3.506	3.522	3.540	3.543	3.547	3.560	3.556	3.543	3.531	3.567
MgO	4.202	4.198	4.198	4.117	4.136	4.141	4.146	4.178	4.175	4.157	4.138	4.207
NaCl	5.541	5.416	5.444	5.500	5.505	5.509	5.514	5.525	5.503	5.487	5.472	5.595
LiCl	5.175	5.107	5.133	5.145	5.147	5.155	5.158	5.165	5.140	5.117	5.115	5.106
Kr	10.86	10.06	10.74	10.79	10.81	10.86	10.86	10.69	10.49	10.05	10.05	9.94
LiF	4.115	4.006	4.030	4.041	4.071	4.073	4.076	4.103	4.098	4.091	4.080	4.010
						All solids						
MARE (%)	1.20	1.37	1.10	1.40	1.37	1.41	1.35	1.25	1.21	1.34	1.54	
MRE (%)	0.68	−1.10	−0.49	−0.47	−0.22	−0.16	−0.03	0.40	0.10	−0.27	−0.62	
						Group I (Ge, Si, GaN, $BaTiO_3$, C)						
MARE (%)	1.15	1.75	1.20	1.44	1.34	1.40	1.32	1.17	1.13	1.33	1.62	
MRE (%)	0.66	−1.27	−0.51	−0.39	−0.20	−0.17	0.00	0.41	0.10	−0.31	−0.74	
						Group II (MgO, NaCl, LiCl, LiF)						
MARE (%)	1.26	0.88	0.99	1.34	1.41	1.41	1.39	1.35	1.32	1.34	1.44	
MRE (%)	0.72	−0.87	−0.47	−0.58	−0.24	−0.14	−0.06	0.38	0.11	−0.22	−0.48	

TABLE IV. Bulk moduli B_0 (GPa) obtained from PBE, HF, PBE0, HSE, and LC calculations. Experimental values are taken from Ref. 93 for Ge; Ref. 41 for Si, β-GaN, C, MgO, NaCl, LiCl, and LiF; Refs. 90 and 91 for $BaTiO_3$; and Ref. 92 for Kr. The calculated MRE and MARE with respect to experimental values are also shown in percent.

	B_0											
	PBE	HF	PBE0	HSE				LC				Expt.
				$\omega = 0.1$	$\omega = 0.2$	$\omega = 0.3$	$\omega = 0.4$	$\omega = 0.1$	$\omega = 0.2$	$\omega = 0.3$	$\omega = 0.4$	
Ge	69.0	76.0	68.8	76.3	75.8	73.3	72.7	71.8	85.3	89.0	95.8	75.8
Si	91.1	116.3	98.1	95.9	93.8	92.0	90.4	90.4	98.0	104.3	109.0	99.2
$BaTiO_3$	146.0	184.0	167.0	164.0	162.0	159.0	156.0	150.0	167.0	166.0	175.0	162.0
β-GaN	173.0	274.6	220.3	215.5	213.3	203.5	189.1	192.2	195.0	218.1	249.3	210.0
C	456.0	534.0	488.0	485.0	483.0	478.0	473.0	469.0	472.0	490.0	508.0	443.0
MgO	152.0	181.0	169.0	166.0	164.0	162.0	160.0	152.0	154.0	161.0	169.0	165.0
NaCl	27.3	32.7	29.3	29.0	28.9	28.7	28.4	28.6	29.1	29.9	30.9	26.6
LiCl	30.7	37.3	33.6	33.6	33.5	33.3	33.1	34.2	36.3	35.1	36.0	35.4
Kr	2.4	6.4	3.8	3.8	3.5	3.1	2.7	3.2	3.5	4.7	5.1	3.4
LiF	67.2	72.0	69.9	69.8	69.8	69.6	69.2	73.1	69.3	67.9	72.0	69.8
All solids												
MARE (%)	8.3	13.7	5.1	3.6	3.4	4.4	5.6	6.6	5.5	6.4	11.2	
MRE (%)	−7.1	13.7	1.7	1.7	0.9	−0.9	−2.6	−2.6	2.0	5.1	11.2	
Group I (Ge, Si, GaN, $BaTiO_3$, C)												
MARE (%)	9.5	16.5	5.7	3.5	3.2	4.7	6.7	7.2	6.1	7.9	15.5	
MRE (%)	−8.3	16.5	1.6	2.1	1.0	−1.5	−4.0	−4.8	2.8	7.9	15.5	
Group II (MgO, NaCl, LiCl, LiF)												
MARE (%)	6.9	10.3	4.5	3.7	3.7	4.0	4.3	5.9	4.8	4.6	5.9	
MRE (%)	−5.6	10.3	1.9	1.1	0.7	0.0	−0.9	0.2	1.1	1.6	5.9	

of the Coulomb interaction depends on the materials. Hence the best treatment of the short-range and long-range parts of the Coulomb interactions should change from material to material. What we have found here is natural in a sense. However, another point we have shown here is that the appropriate choice of ω with each exchange-correlation functional provides reasonable agreement with the calculated band gaps for a rather wide range of materials: HSE with $\omega \sim 0.1 a_B^{-1}$ for materials with band gaps smaller than 7 eV, and LC with $\omega \sim 0.2\, a_B^{-1}$ for materials with band gaps larger than 7 eV. This information certainly provides a practical recipe to obtain reliable band gaps for various materials.

The calculated bandwidths by the PBE functional are in good agreement with the available experimental values (Table II). Other hybrid functionals also provide reasonable agreement, in particular with appropriate choices of the ω parameter for the HSE and LC functionals. On the other hand, the HFA shows a substantial overestimate for each material.

B. Structural properties

We next examinethe performance of the hybrid functionals in describing structural properties. Tables III and IV show calculated lattice constants a_0 and bulk moduli B_0, respectively, of the ten materials. The a_0 and B_0 values are determined by fitting parameters in the Murnaghan equation of state to the calculated total energy as a function of the volume. In MARE and MRE presented in Table III, the calculated value for solid Kr is not included. As shown in this table, the calculated lattice constant of Kr is substantially larger than the experimental value: It is overestimated by 1.1%–9.2% in the GGA and in the hybrid approximations, and by 1.2% in the HFA. This is because the van der Waals interaction, which is unable to be treated in the approximations examined in this paper, plays an essential role in solid Kr. We thus exclude the value for Kr from the statistical assessment. The results obtained by PBE agree reasonably well with the experimental values (MRE = 0.68% and MARE = 1.20% for a_0 and MRE = −7.1% and MARE = 8.3% for B_0). The accuracy of the HFA is slightly inferior to that of PBE (MRE = −1.10% and MARE = 1.37% for a_0 and MRE = 13.7% and MARE = 13.7% for B_0). The PBE0 functional shows better accuracy with the MRE = −0.49% and MARE = 1.10% for a_0, and MRE = −1.7% and MARE = 5.1% for B_0.

The calculated lattice constants using the HSE and LC functionals are insensitive to the choice of ω: The difference obtained from different ω values is within 1%. The difference in the calculated bulk modulus from different ω values is not as small as in the lattice constant, partly because the fitting by the Murnaghan equation is incomplete. For the HSE functional, the value $\omega = 0.1 a_B^{-1}$ produces the best agreement with the experiments: MRE = −0.47% and MARE = 1.40% for a_0, and MRE = 1.7% and MARE = 3.6% for B_0. For the LC functional, we have found that $\omega = 0.2 a_B^{-1}$ produces the best results: MRE = 0.10% and MARE = 1.21% for a_0, and MRE = 2.0% and MARE = 5.5% for B_0. These optimum values for ω for the HSE and LC functionals are identical to the optimum values determined from the calculated MRE and MARE for band gaps, corroborating the appropriate choice of ω.

V. CONCLUSION

We have studied the validity of hybrid exchange-correlation functionals in density functional theory by implementing three hybrid functionals in a well-established plane-wave basis-set code named TAPP and by calculating the structural properties and electron states of ten representative materials in which the experimental energy gaps range from 0.67 to 14.20 eV. The three hybrid exchange-correlation functionals examined in this paper are PBE0 proposed by Perdew, Burke, and Ernzerhoff, HSE proposed by Heyd, Scuseria, and Ernzerhoff, and LC originally proposed by Savin and by Hirao and his collaborators. For comparison, results from the generalized-gradient approximation, i.e., PBE and HFA, have been presented. The ten materials we examined are Ge, Si, GaN, $BaTiO_3$, diamond, MgO, LiCl, NaCl, Kr, and LiF, which are representatives of covalent, ionic, and rare-gas solids.

We have found that structural properties such as the lattice constants are already well reproduced by the PBE functional and also by HFA and that the hybrid functionals show better agreement with the experimental values. We have determined appropriate values of ω in the separation of the short-range and long-range parts in the Coulomb interaction: The optimum value is $\omega = 0.1a_B^{-1}$ for the HSE functional and $\omega = 0.2a_B^{-1}$ for the LC functional. By choosing the appropriate value of ω in the HSE and LC functionals, we have achieved better agreement in the lattice constants and further substantial improvement in the description of elastic constants such as bulk moduli for the ten materials.

Dramatic success of the hybrid functionals was observed in the calculated band gaps. We have found that the calculated band gaps by the LC functional for the wide-band-gap materials agree satisfactorily with the experimental values, with a mean relative error (MRE) of 3.0%, whereas the band gaps by the HSE functional for the small-band-gap materials agree well with the experimental values, with a MRE of 0.7%. This good description of the band gaps is unprecedented in density functional theory, where the LDA and the GGA produce a value with a MRE of approximately 40%–50%, and it is comparable with or better than what the GW approximation produces. The ω value leading to the best agreement with the experiments is $0.1a_B^{-1}$ for the HSE functional and $0.2a_B^{-1}$ for the LC functional. These ω values are identical to the optimum values determined from the examination of the structural properties. The calculated valence-band widths by the hybrid functionals also agree satisfactorily with the experimental values.

It is now established that the HSE and LC functionals with an appropriate choice of the ω parameter are useful to describe the structural and electronic properties of various materials. Rigorous justification of the choice of the form of the hybrid functionals along with a guiding principle of the choice of ω would offer further developments in the first-principles calculations.

ACKNOWLEDGMENTS

The work is partly supported by a grant-in-aid project from MEXT, Japan, "Scientific Research on Innovative Areas: Materials Design through Computics—Complex Correlation and Non-equilibrium Dynamics" under Contract No. 22104005. Computations were done at the Supercomputer Center, Institute for Solid State Physics, University of Tokyo, and at the Research Center for Computational Science, National Institutes of Natural Sciences.

*matsushita@comas.t.u-tokyo.ac.jp

[1] W. Kohn and L. J. Sham, Phys. Rev. **140**, A1133 (1965).
[2] P. Hohenberg and W. Kohn, Phys. Rev. **136**, B864 (1964).
[3] For a review, *Theory of the Inhomogeneous Electron Gas*, edited by S. Lundqvist and N. H. March (Plenum Pres NY, 1983).
[4] T. Asada and K. Terakura, Phys. Rev. B **46**, 13599 (1992), and references therein.
[5] A. Oshiyama, N. Shima, T. Nakayama, K. Shiraishi, and H. Kamimura, in *Mechanisms of High Temperature Superconductivity*, edited by H. Kamimura and A. Oshiyama (Springer-Verlag, 1989), p. 111.
[6] J. P. Perdew and S. Kurth, in *A Premier in Density Functional Theory*, edited by C. Fiolhais, F. Nogueira, and M. A. L. Marques (Springer, Berlin 2003).
[7] For a review, S. Kümmel and L. Kronik, Rev. Mod. Phys. **80**, 3 (2008).
[8] J. P. Perdew, K. Burke, and M. Ernzerhof, Phys. Rev. Lett. **77**, 3865 (1997); **78**, 1396(E) (1997).
[9] J. P. Perdew, A. Ruzsinszky, G. I. Csonka, O. A. Vydrov, G. E. Scuseria, L. A. Constantin, X. Zhou, and K. Burke, Phys. Rev. Lett. **100**, 136406 (2008).
[10] J. P. Perdew, S. Kurth, A. Zupan, and P. Blaha, Phys. Rev. Lett. **82**, 2544 (1999); **82**, 5179(E) (1999).
[11] T. Van Voorhis and G. E. Scuseria, J. Chem. Phys. **109**, 400 (1998).
[12] J. Tao, J. P. Perdew, V. N. Staroverov, and G. E. Scuseria, Phys. Rev. Lett. **91**, 146401 (2003).
[13] V. N. Staroverov, G. E. Scuseria, J. Tao, and J. P. Perdew, J. Chem. Phys. **119**, 12129 (2003); **121**, 11507(E) (2004).
[14] J. P. Perdew and A. Zunger, Phys. Rev. B **23**, 5048 (1981).
[15] A. J. Cohen, P. Mori-Sánchez, and W. Yang, Science **321**, 721 (2008).
[16] O. A. Vydrov and G. E. Scuseria, J. Chem. Phys. **121**, 8187 (2004).
[17] A. Ruzsinszky, J. P. Perdew, G. I. Csonka, O. A. Vydrov, and G. E. Scuseria, J. Chem. Phys. **125**, 194112 (2006).
[18] A. Ruzsinszky, J. P. Perdew, G. I. Csonka, O. A. Vydrov, and G. E. Scuseria, J. Chem. Phys. **126**, 104102 (2007).
[19] J. P. Perdew, A. Ruzsinszky, G. I. Csonka, O. A. Vydrov, G. E. Scuseria, V. N. Staroverov, and J. Tao, Phys. Rev. A **76**, 040501 (2007).
[20] J. P. Perdew, R. G. Parr, M. Levy, and J. L. Balduz Jr., Phys. Rev. Lett. **49**, 1691 (1982).
[21] J. P. Perdew and M. Levy, Phys. Rev. Lett. **51**, 1884 (1983).
[22] L. J. Sham and M. Schlüter, Phys. Rev. Lett. **51**, 1888 (1983).

[23]L. J. Sham and M. Schlüter, Phys. Rev. B **32**, 3883 (1985).
[24]J. F. Janak, Phys. Rev. B **18**, 7165 (1978).
[25]P. Mori-Sánchez, A. J. Cohen, and W. Yang, Phys. Rev. Lett. **100**, 146401 (2008).
[26]A. J. Cohen, P. Mori-Sánchez, and W. Yang, Phys. Rev. B **77**, 115123 (2008).
[27]J. D. Talman and W. F. Shadwick, Phys. Rev. A **14**, 36 (1976).
[28]S. Ivanov, S. Hirata, and R. J. Bartlett, Phys. Rev. Lett. **83**, 5455 (1999).
[29]A. Görling, Phys. Rev. Lett. **83**, 5459 (1999).
[30]W. Yang and Q. Wu, Phys. Rev. Lett. **89**, 143002 (2002).
[31]A. Becke, J. Chem. Phys. **98**, 1372 (1993).
[32]A. Becke, J. Chem. Phys. **98**, 5648 (1993).
[33]See, e.g., P. J. Stephens, F. J. Devlin, C. F. Chabalowski, and M. J. Frisch, J. Phys. Chem. **98**, 11623 (1994); R. H. Hertwig and W. Koch, Chem. Phys. Lett. **268**, 345 (1997); S. F. Sousa, P. A. Fernandes, and M. J. Ramos, J. Phys. Chem. A **111**, 10439 (2007).
[34]J. P. Perdew, M. Ernzerhof, and K. Burke, J. Chem. Phys. **105**, 9982 (1996).
[35]O. Gunnarsson and B. I. Lundqvist, Phys. Rev. B **13**, 4274 (1976).
[36]M. Ernzerhof and G. E. Scuseria, J. Chem. Phys. **110**, 5029 (1999).
[37]C. Adamo and V. Barone, J. Chem. Phys. **110**, 6158 (1999).
[38]D. M. Bylander and L. Kleinman, Phys. Rev. B **41**, 7868 (1990).
[39]J. Heyd, G. E. Scuseria, and M. Ernzerhof, J. Chem. Phys. **118**, 8207 (2003); **124**, 219906(E) (2006).
[40]H. Stoll and A. Savin, *Density Functional Methods in Physics* (Plenum, New York, 1985), pp. 177.
[41]J. Heyd and G. E. Scuseria, J. Chem. Phys. **121**, 1187 (2004).
[42]J. Heyd, J. E. Peralta, G. E. Scuseria, and R. L. Martin, J. Chem. Phys. **123**, 174101 (2005).
[43]V. Barone, J. E. Peralta, M. Wert, J. Heyd, and G. Scuseria, Nano Lett. **5**, 1621 (2005).
[44]J. E. Peralta, J. Heyd, G. E. Scuseria, and R. L. Martin, Phys. Rev. B **74**, 073101 (2006).
[45]J. Paier, M. Marsman, K. Hummer, G. Kresse, I. C. Gerber and J. G. Ángyán, J. Chem. Phys. **124**, 154709 (2006).
[46]M. Marsman, J. Paier, A. Stroppa, and G. Kresse, J. Phys. Condens. Matter **20**, 064201 (2008).
[47]E. R. Batista, J. Heyd, R. G. Hennig, B. P. Uberuaga, R. L. Martin, G. E. Scuseria, C. J. Umrigar, and J. W. Wilkins, Phys. Rev. B **74**, 121102(R) (2006).
[48]F. Fuchs, J. Furthmüller, F. Bechstedt, M. Shishkin, and G. Kresse, Phys. Rev. B **76**, 115109 (2007).
[49]A. Stroppa and G. Kresse, New J. Phys. **10**, 063020 (2008).
[50]E. N. Brothers, A. F. Izmaylov, J. O. Normand, V. Barone, and G. E. Scuseria, J. Chem. Phys. **129**, 011102 (2008).
[51]H. Leininger, H. Stoll, H.-J. Werner, and A. Savin, Chem. Phys. Lett. **275**, 151 (1997).
[52]A. Savin, *Recent Developmennts and Applications of Modern Density Functional Theory* (Elsevier, 1996) pp.327–357.
[53]H. Iikura, T. Tsuneda, T. Yanai, and K. Hirao, J. Chem. Phys. **115**, 3540 (2001).
[54]M. Kamiya, T. Tsuneda, and K. Hirao, J. Chem. Phys. **117**, 6010 (2002).
[55]Y. Tawada, T. Tsuneda, S. Yanagisawa, T. Yanai, and K. Hirao, J. Chem. Phys. **120**, 8425 (2004).
[56]M. Chiba, T. Tsuneda, and K. Hirao, J. Chem. Phys. **124**, 144106 (2006).
[57]H. Sekino, Y. Maeda, M. Kamiya, and K. Hirao, J. Chem. Phys. **126**, 014107 (2007).
[58]O. A. Vydrov, J. Heyd, A. V. Krukau, and G. E. Scuseria, J. Chem. Phys. **125**, 074106 (2006).
[59]O. A. Vydrov and G. E. Scuseria, J. Chem. Phys. **125**, 234109 (2006).
[60]O. A. Vydrov, G. E. Scuseria, and J. P. Perdew, J. Chem. Phys. **126**, 154109 (2007).
[61]I. C. Gerber, J. G. Angyan, M. Marsman, and G. Kresse, J. Chem. Phys. **127**, 054101 (2007).
[62]Tokyo Ab-initio Program Package (TAPP) has been developed by a consortium initiated at the University of Tokyo.
[63]O. Sugino and A. Oshiyama, Phys. Rev. Lett. **68**, 1858 (1992).
[64]J. Yamauchi, M. Tsukada, S. Watanabe, and O. Sugino, Phys. Rev. B **54**, 5586 (1996).
[65]H. Kageshima and K. Shiraishi, Phys. Rev. B **56**, 14985 (1997).
[66]J. Heyd and G. E. Scuseria, J. Chem. Phys. **120**, 7274 (2004).
[67]T. M. Henderson, A. F. Izmaylov, G. Scalmani, and G. E. Scuseria, J. Chem. Phys. **131**, 044108 (2009).
[68]N. Troullier and J. L. Martins, Phys. Rev. B **43**, 1993 (1991).
[69]D. Vanderbilt, Phys. Rev. B **41**, 7892 (1990).
[70]F. Gygi and A. Baldereschi, Phys. Rev. B **34**, 4405 (1986).
[71]B. Wenzien, G. Cappellini, and F. Bechstedt, Phys. Rev. B **51**, 14701 (1995).
[72]P. Carrier and G. A. Voth, J. Chem. Phys. **108**, 4697 (1998).
[73]J. Spencer and A. Alavi, Phys. Rev. B **77**, 193110 (2008).
[74]M. Ernzerhof and J. P. Perdew, J. Chem. Phys. **109**, 3313 (1998)
[75]J. Heyd, Ph. D. thesis, Rice University, 2004.
[76]S. G. Louie, S. Froyen, and M. L. Cohen, Phys. Rev. B **26**, 1738 (1982).
[77]M. S. Hybertsen and S. G. Louie, Phys. Rev. B **34**, 5390 (1986).
[78]F. Aryasetiawan and O. Gunnarsson, Rep. Prog. Phys. **61**, 237 (1998).
[79]For discussion on several ambiguities in the *GW* approximation, see M. L. Tiago, S. Ismail-Beigi, and S. G. Louie, Phys. Rev. B **69**, 125212 (2004); M. van Schilfgaarde, T. Kotani, and S. V. Faleev, *ibid.* **74**, 245125 (2006), and references therein.
[80]*Zahlenwerte und Funktionen aus Naturwissenschaften und Technik*, in vol. III of Landolt-Bornstein (Springer, New York, 1982), pt. 17a.
[81]S. H. Wemple, Phys. Rev. B **2**, 2679 (1970).
[82]S. Adachi, *Optical Properties of Crystalline and Amorphous Semiconductors: Numerical Data and Graphical Information* (Kluwer Academic, Dordrecht, 1999).
[83]R. T. Poole, J. Liesegang, R. C. G. Leckey, and J. G. Jenkin, Phys. Rev. B **11**, 5190 (1975).
[84]R. J. Magyar, A. Fleszar, and E. K. U. Gross, Phys. Rev. B **69**, 045111 (2004).
[85]M. Rohlfing and S. G. Louie, Phys. Rev. B **62**, 4927 (2000).
[86]A. L. Wachs, T. Miller, T. C. Hsieh, A. P. Shapiro, and T. C. Chiang, Phys. Rev. B **32**, 2326 (1985).
[87]F. R. McFeely *et al.*, Phys. Rev. B **9**, 5268 (1974).
[88]F. J. Himpsel, J. F. van der Veen, and D. E. Eastman, Phys. Rev. B **22**, 1967 (1980).

[89] Superiority of HSE over GGA has been recognized from Gaussian-orbital-basis calculations. For reviews, B. G. Janesko, T. M. Henderson, and G. E. Scuseria, Phys. Chem. Chem. Phys. **11**, 443 (2009); T. M. Henderson, J. Paier, and G. E. Scuseria, Phys. status solidi B **248**, 767 (2011).

[90] S. Piskunov, E. Heifetsb, R. I. Eglitisa, and G. Borstel, Comput. Mater. Sci. **29**, 165 (2004).

[91] *Ferroelectrics and Related Substances* edited byK. H. Hellwege and A. M. Hellwege, Landolt-Bornstein New Series, Vol. 3, Group III (Springer Verlag, Berlin 1969).

[92] P. Varotsos and K. Alexopoulos, Phys. Rev. B **15**, 4111 (1977).

[93] A. R. Jivani, P. N. Gajjar, and A. R. Jani, Semicond. Phys. Quantum. **5**, 243 (2002).